




Genome-Scale Investigation of the Metabolic Determinants Generating Bacterial Fastidious Growth

Léo Gerlin,^a Ludovic Cottret,^a Sophie Cesbron,^b Géraldine Taghouti,^b Marie-Agnès Jacques,^b  Stéphane Genin,^a  Caroline Baroukh^a

^aLIPM, Université de Toulouse, INRAE, CNRS, Castanet-Tolosan, France

^bIRHS, INRAE, AGROCAMPUS-Ouest, Université d'Angers, Beaucouzé, France

ABSTRACT High proliferation rate and robustness are vital characteristics of bacterial pathogens that successfully colonize their hosts. The observation of drastically slow growth in some pathogens is thus paradoxical and remains unexplained. In this study, we sought to understand the slow (fastidious) growth of the plant pathogen *Xylella fastidiosa*. Using genome-scale metabolic network reconstruction, modeling, and experimental validation, we explored its metabolic capabilities. Despite genome reduction and slow growth, the pathogen's metabolic network is complete but strikingly minimalist and lacking in robustness. Most alternative reactions were missing, especially those favoring fast growth, and were replaced by less efficient paths. We also found that the production of some virulence factors imposes a heavy burden on growth. Interestingly, some specific determinants of fastidious growth were also found in other slow-growing pathogens, enriching the view that these metabolic peculiarities are a pathogenicity strategy to remain at a low population level.

IMPORTANCE *Xylella fastidiosa* is one of the most important threats to plant health worldwide, causing disease in the Americas on a range of agricultural crops and trees, and recently associated with a critical epidemic affecting olive trees in Europe. A main challenge for the detection of the pathogen and the development of physiological studies is its fastidious growth, as the generation time can vary from 10 to 100 h for some strains. This physiological peculiarity is shared with several human pathogens and is poorly understood. We performed an analysis of the metabolic capabilities of *X. fastidiosa* through a genome-scale metabolic model of the bacterium. This model was reconstructed and manually curated using experiments and bibliographical evidence. Our study revealed that fastidious growth most probably results from different metabolic specificities such as the absence of highly efficient enzymes or a global inefficiency in virulence factor production. These results support the idea that the fragility of the metabolic network may have been shaped during evolution to lead to the self-limiting behavior of *X. fastidiosa*.

KEYWORDS metabolic network, metabolic pathways, metabolic modeling, robustness, pathogen, growth, *Xylella fastidiosa*, *Xanthomonas*, fastidious


Optimal growth rate and robustness against environmental perturbations are major properties contributing to bacterial fitness (1–3). For example, experimental evolution of the plant pathogen *Ralstonia solanacearum* on several hosts revealed that bacteria acquired both enhanced growth rate and better robustness through enlarged catabolic capacities, showing that these phenotypes are under selective pressure (4, 5). The robustness of virulence functions in this pathogen is also illustrated by the plethora of effectors transiting through the type 3 secretion system, as well as for the regulatory and metabolic networks (6, 7). These traits were shown to be crucial to invade the host and bypass its immune system (7, 8). However, it is also well documented that some

Citation Gerlin L, Cottret L, Cesbron S, Taghouti G, Jacques M-A, Genin S, Baroukh C. 2020. Genome-scale investigation of the metabolic determinants generating bacterial fastidious growth. *mSystems* 5:e00698-19. <https://doi.org/10.1128/mSystems.00698-19>.

Editor Joshua E. Elias, Chan Zuckerberg Biohub

Copyright © 2020 Gerlin et al. This is an open-access article distributed under the terms of the [Creative Commons Attribution 4.0 International license](https://creativecommons.org/licenses/by/4.0/).

Address correspondence to Stéphane Genin, stephane.genin@inrae.fr, or Caroline Baroukh, caroline.baroukh@inrae.fr.

 Why is #Xylellafastidiosa "fastidious"? Genome-scale metabolic modeling unraveled specificities that could explain the slow-growing phenotype of the pathogen. This phenotype could be a pathogenicity strategy.

Received 23 October 2019

Accepted 5 March 2020

Published 31 March 2020

TABLE 1 Comparison of metabolic networks

Network characteristic	No. of reactions	No. of metabolites
<i>E. coli</i>	2,583	1,805
<i>R. solanacearum</i>	2,644	2,574
<i>B. pertussis</i>	1,203	1,143
<i>X. fastidiosa</i>	1,158	1,107

bacterial pathogens are slow growing, qualified as fastidious, such as *Legionella* species (9), *Brucella* species (9), and *Bordetella pertussis* (10–12). Fastidiousness refers to an arduous laboratory handling, and these difficulties were first hypothesized as a consequence of a lack of knowledge of nutritional and environmental requirements. However, later studies reported that fastidiousness is mostly, or complementarily, related to an intrinsic slow growth (13, 14) which could not be overcome by optimized culture medium (13).

Xylella fastidiosa is the infectious agent of several diseases affecting plants of agronomical interest (15). This threatening bacterium is transmitted through xylem-sap-feeding insect vectors (15). Once inside the xylem capillary vessels, *X. fastidiosa* spreads, grows, produces virulence factors like exopolysaccharides (EPS), and forms biofilms (15, 16) before colonizing the foregut of a new insect host (15). *X. fastidiosa*'s fastidious growth was reported both *in vitro* and *in planta* and is responsible for its difficult isolation (17). Design of synthetic growth medium was carried out (18–20), but after nearly 2 decades of medium optimization, the persisting difficulty of growing *X. fastidiosa*, with a doubling time in the range of 100 h for some strains (19, 21), brings out that the slow growth is a property of the organism. As the genome size of the bacterium is severely reduced, it is tempting to speculate that part of the metabolic robustness is lost in *X. fastidiosa*. To understand the metabolic factors at the origin of fastidious growth, and the level of robustness of the bacterium, we reconstructed a high-quality genome-scale metabolic network of *X. fastidiosa*, based on genomic and experimental data. This network allowed us to explore the metabolic capabilities of *X. fastidiosa*. We unraveled a lack of metabolic robustness to sustain growth through flux variability, enzyme redundancy, gene deletion, and trophic capabilities, supported by both modeling and experiments. We then sought to deduce some metabolic determinants of fastidious growth. We found that loss of robustness mostly affected efficient parts of the network, such as enzymes with high catalytic activities, or central reactions which are assumed to play a crucial role in growth. Thereby, we unraveled that *X. fastidiosa* metabolism mostly relies on pathways and reactions which cannot ensure a fast proliferation. We demonstrated that the global network has a weak metabolic yield in producing central virulence factor, thus showing that it is structurally inefficient, which could also severely impair growth.

RESULTS

The metabolic network of *X. fastidiosa*. We built a genome-scale metabolic network of *X. fastidiosa* (see Data Set S1, Text S1, and Text S2 in the supplemental material) using in-house automatic reconstruction algorithms (22) from the genomic sequence of *Xylella fastidiosa* subsp. *multiplex* strain CFBP 8418 isolated in 2015 in Corsica (23). A manual curation of each reaction was then performed using databases, literature, and simulations. Novel reactions were written to take into account the biosynthesis of EPS and lipopolysaccharides (LPS) (24–26). To represent the global cost of excreted proteins, which are crucial virulence factors, we included reactions for the biosynthesis and excretion of a proteic virulence factor through the type II secretion system (27). The reconstruction process is summarized in Data Set S2.

The final numbers of reactions and metabolites of the *X. fastidiosa* network (Table 1) are remarkably small compared to *Escherichia coli* and *R. solanacearum*. However, all the core carbon and nitrogen reactions from the central metabolism were found (except one enzyme; see below), as well as the biosynthesis of all vital compounds (Fig. 1A). The

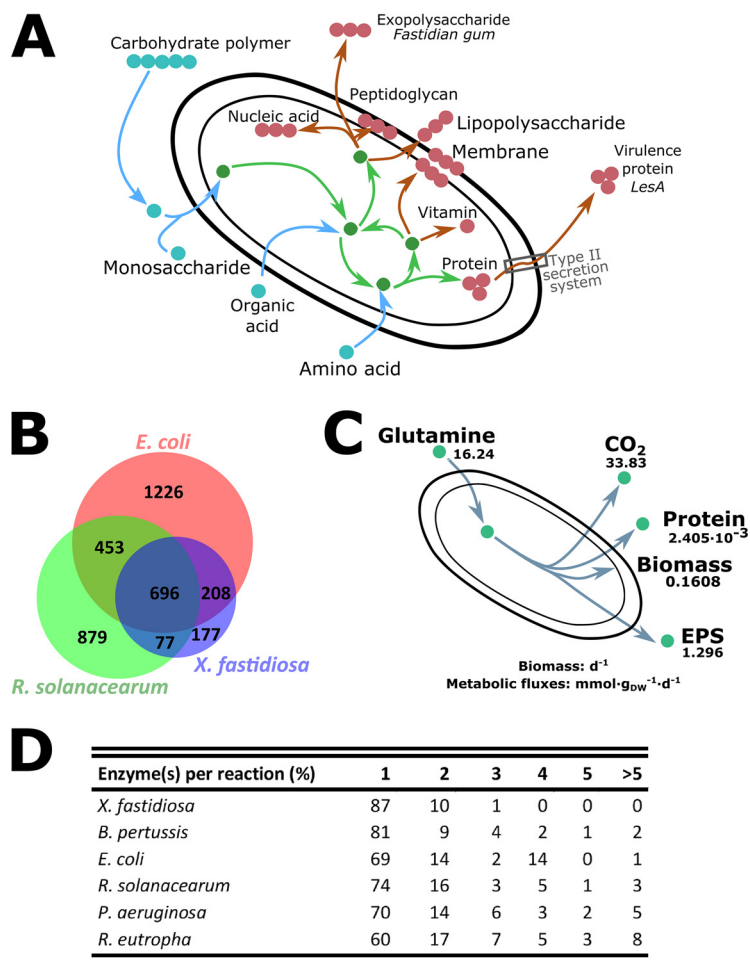


FIG 1 General characteristics of the reconstructed metabolic network. (A) Global overview of the reconstructed metabolic pathways in *Xylella fastidiosa*. This schema highlights the metabolic behaviors of *Xylella fastidiosa*. For catabolism (external substrates and catabolic reactions in blue), *X. fastidiosa* is able to degrade polymers and assimilate them or catabolize elements from xylem sap such as amino acids and organic acids. Central metabolites and reactions are schematized in green (glycolysis and TCA cycle). Metabolites/reactions in red/brown highlight anabolic capabilities: the production of biomass macromolecules (membranes, lipopolysaccharides, peptidoglycans, vitamins, proteins, and nucleic acids) and the secretion of virulence factors (virulence protein through the type II secretion system and fastidian gum [EPS]). (B) Venn diagram depicting the number of metabolic reactions in *E. coli*, *R. solanacearum*, and *X. fastidiosa*. The lists of the reactions found in each part of the Venn diagram are available in Data Set S2. (C) Inputs and outputs of an FBA simulation of *X. fastidiosa* growth on glutamine under conditions close to experimental conditions. The objective function of FBA was minimization of glutamine import. Growth and production rates were calculated from previous publications (19, 82). Flux values are in mmol·g (DW)⁻¹·day⁻¹ for all inputs/outputs except for biomass (day⁻¹). See Text S3 for the constraints used for the simulation and Data Set S2 for the FBA solution. Scripts are available on <https://github.com/lgerlin/xfas-metabolic-model>. (D) Distribution of the number of enzymes for each metabolic reaction in *X. fastidiosa* and metabolic models from other bacteria. Proportions of reactions carried out by 1, 2, 3, 4, 5, and >5 enzymes were computed for each metabolic model. The complete data are available in Data Set S2.

precursors for the specific macromolecules EPS and LPS, which are key virulence determinants (28), can also be synthesized.

We performed genome sequence comparisons between *X. fastidiosa* subsp. *multiplex* strain CFBP 8418, *Xylella fastidiosa* subsp. *pauca* strain 9a5c (isolated from citrus in Brazil) (29), and *Xylella fastidiosa* subsp. *fastidiosa* strain Temecula1 (isolated from grapevine in California) (30) to estimate the metabolic network conservation between the three subspecies (Table S1 and Table S2). Because these differential reactions represented 1% or less of the network, with most of them being not connected to central metabolism, we concluded that the architecture of the metabolic networks is

probably highly similar between these three *X. fastidiosa* subspecies. Therefore, the conclusions drawn in the following sections on strain CFBP 8418 extend to at least three subspecies of *X. fastidiosa*.

Predicted metabolic capacities of *X. fastidiosa*. The comparison of the number of metabolic reactions shared between *X. fastidiosa*, *E. coli*, and *R. solanacearum* revealed that *X. fastidiosa* has undergone a strong metabolic reduction, which is associated with its reduced genome size, and illustrated by the decreased numbers of reactions that are specific to *X. fastidiosa* (Fig. 1B). The complete list of shared or specific reactions is available in Data Set S2. The metabolic core shared between the three organisms was around 700 reactions, which represents 58% of the *X. fastidiosa* model. *E. coli* shares a wide range of reactions with *X. fastidiosa*, including vitamin biosynthesis and transport processes. *X. fastidiosa* and *R. solanacearum* have fewer reactions in common, probably due to their more distant phylogenetic relationship (beta- versus gammaproteobacteria). Among them, we identified several metabolic pathways related to *in planta* lifestyle and pathogenicity such as nitrilase (EC 3.5.5) reactions, which detoxify nitriles (31), and peroxidases (EC 1.11.1) degrading radical oxygen species (ROS) (32), both nitriles and ROS being produced by plants upon infection (32, 33). These two plant pathogens also shared degradation reactions for plant polymers like pectin.

The comparative analysis revealed a large number of reactions (450) absent only in *X. fastidiosa*. Several of them are related to lipid metabolism, such as the pathway to use lipid as carbon source (β -oxidation) and to alternate carbon metabolism reactions, which enable the use of diverse compounds as carbon source, like carbohydrates (e.g., tagatose and glycogen) or small organic molecules (e.g., benzoate, D-galacturonate, and phenylacetate). These findings highlighted that *X. fastidiosa* metabolism appears limited in terms of metabolic diversity.

Although *X. fastidiosa* possesses all the vital vitamin and cofactor biosynthetic pathways, it lacks several related pathways that are generally found in fast-growing bacteria. For instance, the couple ubiquinone-8/ubiquinol-8 was the only redox couple from the quinone group found to be synthesized. In contrast to *R. solanacearum*, no cobalamin (vitamin B₁₂) biosynthesis is possible. Accordingly, *X. fastidiosa* uses only enzymes with no requirement for cobalamin, which cannot be found in plants (34). We observed a similar case for molybdopterin, which forms the molybdenum cofactor.

Previous studies suggested that *X. fastidiosa* was limited in aerobic respiration, because no cytochromes with a high affinity for O₂ were found in the genome sequences (35). The absence of cytochrome *c* oxidase was also reported, limiting the aerobic respiration to cytochrome *bo*₃ ubiquinone oxidase (EC 1.10.3.10). It was thus suggested that the bacterium preferentially uses anaerobic respiration (35). Contrary to this hypothesis, no complete anaerobic respiration was found to be functional in the metabolic network, which supports the view of a functional and favored aerobic respiration in *X. fastidiosa*. However, the limitation of aerobic respiration suggests that the bacterium is also limited in its respiratory system.

Succinate dehydrogenase (EC 1.3.99.1), an enzyme from central and respiratory metabolism composed of four subunits, was also found to have lost a membrane subunit in *X. fastidiosa*. This enzymatic complex was reported to be functional with only one membrane domain (36). We thus expect that the metabolic reactions can occur in *X. fastidiosa* but might also be less efficient than the complete form of the enzyme complex.

Our primary analysis of the network structure showed that the core metabolism is complete, and its functionality was confirmed by flux balance analysis (FBA) simulations (Fig. 1C and Data Set S2), accepting the fact that an FBPase activity exists (see below). Simulation (Data Set S2) results show that all biomass components can be produced from the tested carbon source, glutamine, a major component of xylem sap (37–40). The majority of glutamine uptake is converted into glutamate (95% of carbon uptake) and then into α -ketoglutarate. α -Ketoglutarate is then converted through the citric acid cycle (tricarboxylic acid [TCA] cycle) to malate and oxaloacetate. Yet, the TCA cycle is

not cyclic. The branch converting oxaloacetate to citric acid is not used, which could be expected for growth in minimal medium with glutamine as sole carbon source. The part of the citric acid cycle used generates central metabolites such as succinyl coenzyme A (CoA) and oxaloacetate. Pyruvate is generated from the citric acid cycle metabolite oxaloacetate, through oxaloacetate decarboxylase (EC 4.1.1.3, 22% of carbon uptake) and malic enzyme (EC 1.1.1.40, 34% of carbon uptake). Finally, these central metabolites are used to generate biomass and virulence factors (EPS and virulence proteins), and the remaining carbon is wasted during metabolic processes as CO₂, more than half through the TCA cycle. NADH is also mainly synthesized thanks to the TCA cycle and ATP through oxidative phosphorylation.

The core central metabolism from *X. fastidiosa* appears to be conserved and functional, although it seems to have lost several pathways compared to other bacteria. These losses do not affect the survival of the bacterium but tend to restrict it to a limited diversity of metabolic behaviors, and probably to a slow and inefficient growth.

Unexpected features in *X. fastidiosa* metabolism. A deeper analysis of the *X. fastidiosa* metabolism revealed the surprising lack of some enzymes which are generally ubiquitous in bacteria. First, no gene was identified to code for fructose-1,6-bisphosphatase (FBPase) (EC 3.1.3.11), despite intensive homology searches with query sequences from a wide range of organisms. The absence of the corresponding gene in strain CFBP 8418, as well as all the other available genomes of *X. fastidiosa*, suggested that these bacteria are not able to perform gluconeogenesis. We verified *in silico* that in our metabolic network, gluconeogenesis was not functional; a precursor such as glutamine could not be converted into glucose with no FBPase. It would imply that *X. fastidiosa* can grow only in the presence of a hexose or a hexose polymer (41, 42), but that was invalidated experimentally (see below and Table 2). Therefore, conversion of fructose-1,6-bisphosphate into fructose-6-phosphate must be achieved by an alternative and previously uncharacterized route.

Strikingly, the pentose phosphate pathway also lacks two of its enzymes: the 6-phosphogluconate dehydrogenase (EC 1.1.1.44) and the transaldolase (EC 2.2.1.2). The absence of 6-phosphogluconate dehydrogenase was already reported in other prokaryotes (43), and its product ribulose 5-phosphate could be rescued through the Entner-Doudoroff pathway. However, the absence of the transaldolase is more surprising, since the enzyme is well conserved in prokaryotes (43).

Experimental validation of carbon source usage. In order to validate the metabolic model predictions, we experimentally assessed the growth of *X. fastidiosa* on 190 potential carbon (C) sources using Biolog phenotype microarrays (PMs); 8 can provide relatively fast growth and 18 can provide relatively slow growth at the scale of *X. fastidiosa* fastidious growth (Table 2). Growth is achievable on diverse xylem fluid components, including five amino acids, citric acid, and D-fructose, even though, surprisingly, eight compounds leading to fast growth are not major components. The number of carbon sources identified using Biolog PMs was 25, which is considerably lower than the number of C sources identified in *R. solanacearum* and *E. coli* (respectively, 36 and 86) (22, 44), confirming our prediction of reduced metabolic diversity. We also used FBA to predict the relative growth rate of *X. fastidiosa* on several substrates. Relative *in silico* growth rates were determined by computing the ratio between the growth rate and the highest growth rate obtained (on glycerol). The discrepancies observed between experimental and simulation results (growth *in vivo* but not predicted *in silico*) were used to correct the network, by adding the missing metabolic reactions for 12 substrates (as specified in the final metabolic network in Data Set S1). The refined metabolic network predicted growth on 24 of the 26 experimentally verified substrates; growth was observed with Biolog PMs on D,L- α -glycerol phosphate and 3-O- β -D-galactopyranosyl-D-arabinose but not modeled because there are no assimilation reactions for these substrates in available metabolic models. Based on the FBA results, we classified the different carbon sources (Table 2 and Data Set S3) by defining relatively fast growth *in silico* as >75% of the maximal growth rate. Sixteen of

TABLE 2 *In silico* and *in vivo* growth assays on different carbon sources using FBA and Biolog PMs

Substrate	Growth assessment		Presence of compound in xylem ^c	
	<i>In silico</i> ^a	Exptl ^b	Grapevine	Olive tree
Amino acids				
L-Proline	+	++	Minor	Minor
L-Glutamate	+	+	ND	Minor
L-Aspartate	+	+	ND	Minor
L-Alanine	+	+	Minor	Minor
L-Glutamine	+	+	Major	Major
L-Arginine	+	+	Minor	Minor
L-Histidine	+	+	Minor	ND
L-Ornithine	+	+	ND	ND
γ-Aminobutyric acid	+	+	ND	Minor
Organic acids				
Acetic acid	+	+	ND	Minor
Citric acid	+	+	Major	ND
Pyruvic acid	+	++	ND	ND
Monosaccharides				
D-Glucose	++	++	Minor	Major
D-Galactose	++	++	ND	ND
D-Trehalose	++	++	ND	ND
D-Fructose	++	+	Minor	Major
D-Ribose	+	+	ND	ND
D-Mannose	++	+	ND	ND
D-Xylose	+	+	ND	ND
Others				
Chitin	++	++/+*	ND	ND
Dextrin	++	+	ND	ND
myo-Inositol	+	++	ND	Minor
Glycerol	++	++	ND	ND
D-Glucosamine	++	+	ND	ND
3-O-β-D-Galactopyranosyl-D-arabinose	Unknown	+	ND	ND
DL-α-Glycerol phosphate	Unknown	+	ND	ND

^aRelative *in silico* growth rates were determined by computing the ratio between the growth rate and the highest growth rate obtained (on glycerol). If the relative *in silico* growth rate was >75%, growth was assessed as relatively fast (++), and if the relative *in silico* growth rate was ≤75%, growth was assessed as relatively slow (+).

^bGrowth assessment was made using Biolog PM respiration rate: ++ for relatively fast growth, referring to a respiration rate above 0.125 h⁻¹, and + for relatively slow growth, referring to a respiration rate under 0.125 h⁻¹ (see Materials and Methods and Data Set S3), except for chitin (*), for which growth was previously determined experimentally (45). Growth was observed with Biolog PMs on D,L-α-glycerol phosphate and 3-O-β-D-galactopyranosyl-D-arabinose but not modeled, because there are no assimilation reactions for these substrates in available metabolic models. Substrates with indeterminate growth or no growth are listed in Data Set S3.

^cXylem fluid composition from grapevine and olive tree was extracted from the work of Andersen and Brodbeck (37) and Montes Borrego et al. (39). Major, concentration ≥ 500 μM; minor, concentration < 500 μM; ND, not detected.

23 (70%) of the predictions were in accordance with the experimental measurements. The highest predicted growth rate was observed with glycerol, and this was confirmed experimentally.

We also tested *in silico* the growth on chitin, a polymer composing the insect foregut wall, not present on Biolog PM plates. A recent study showed the necessity of a chitinase (ChiA) for both insect and plant colonization and suggested that chitin is the favored carbon source in the insect environment (45). Our results (Table 2) support the hypothesis that chitin is a favored substrate since it provides some of the fastest growth (relatively speaking for *X. fastidiosa*).

Modeling-based evidence for a fragile metabolism. To first estimate the level of functional redundancy in the *X. fastidiosa* network, we determined the number of enzymes associated with each reaction in comparison with other reference metabolic models (Fig. 1D and Data Set S2). Eighty-seven percent of the metabolic reactions in *X. fastidiosa* are carried out by a unique enzyme, while no other organism exceeds 80% except the also-fastidious *Bordetella pertussis* (11). Alternative enzymes are indicative of functional redundancies in the network and are generally associated with environmen-

TABLE 3 Simulation analyses of the metabolic network

Organism	Proportion (%) of:			
	Essential metabolic genes (gene essentiality ^a) in:		Reactions (flux variability ^b)	
	Glucose medium	Protein-rich environment	Varying	Bidirectional
<i>E. coli</i>	15	12	60	4
<i>R. solanacearum</i>	15	13	48	3
<i>B. pertussis</i>	No growth	40		
<i>X. fastidiosa</i>	54	51	32	1

^aProportion of essential metabolic genes according to metabolic modeling, in glucose medium and a protein-rich environment. As *B. pertussis* cannot grow on glucose, the gene essentiality value is given only for a simulated protein-rich growth environment (12). Data for *B. pertussis* and *E. coli* (growth on glucose) were extracted from the work of Fyson et al. (12) and Orth et al. (67). Values for *R. solanacearum* and *X. fastidiosa* in both environments and for *E. coli* in a protein-rich environment were computed for this study. The detailed results are available in Data Set S4.

^bAssessment of flux variability. The proportion of varying reactions represents the number of reactions with non-null flux variation divided by the total number of metabolic reactions in the network. Bidirectional reactions are reversible reactions that can carry out both positive and negative flux to sustain an optimal growth. The proportion was equally determined by calculating the ratio of these reactions divided by the total number of metabolic reactions in the network. The detailed results are available in Data Set S2.

tal plasticity. This lack in *X. fastidiosa* illustrated further the low flexibility of its metabolism. We then performed a gene essentiality analysis on the network. The results for *X. fastidiosa* and other reference organisms are presented in Table 3 (detailed information in Data Set S4). Strikingly, the predicted proportion of essential genes was 54% on glucose and 51% in a protein-rich environment, which is considerably higher than the other tested bacteria. This outstandingly high proportion of essential genes in *X. fastidiosa* illustrates the fragility of the metabolic network against perturbations.

Fragility and low flexibility of *X. fastidiosa* metabolism were confirmed using flux variability analysis (FVA). FVA is an *in silico* analysis to estimate if alternative flux values, due to an internal or external perturbation, will still sustain an optimal metabolic behavior. We performed FVA using L-glutamine as carbon source and growth as the objective function. Similar analyses were also conducted with *E. coli* and *R. solanacearum* (Table 3 and Data Set S2). As expected from the previous results, the proportion of varying reactions (i.e., reactions with alternative fluxes able to sustain the biological objective) was significantly lower (32%) in *X. fastidiosa* than in *R. solanacearum* (48%) and *E. coli* (60%). Thus, only a limited proportion of the metabolic reactions can still sustain optimal growth if their fluxes vary. This particular trait confirmed a lack of flexibility in *X. fastidiosa* metabolism.

A higher cost for virulence can compromise *X. fastidiosa* growth. We finally assessed the efficiency of the network structure for a specific task by determining metabolic yields on proliferation and on virulence factors. Metabolic yields were defined as the maximal proportion of carbon which could be invested in the biosynthesis of a specific macromolecule (virulence factor) or biomass. The obtained efficiency data are presented in Table 4 and compared to another plant pathogen, *R. solanacearum*. This other plant pathogen also has a network including virulence proteins

TABLE 4 Structural efficiency analysis of *X. fastidiosa* and *R. solanacearum* metabolic models^a

Biological objective	Yield (%) for species:	
	<i>Xylella fastidiosa</i>	<i>Ralstonia solanacearum</i>
Biomass	54	58
Protein	61	64
EPS	58	72

^aMetabolic yields were compared for different biological objectives: (i) production of biomass, (ii) production of virulence proteins, and (iii) production of EPS. The mathematical details on yield determination are given in Data Set S2.

and EPS secretion in the model, in contrast to other metabolic models including *E. coli*. The comparison was thus limited to these two plant pathogens.

Similar efficiency is observed for biomass production and extracellular protein secretion (Table 4; Data Set S2). However, the structure of the *X. fastidiosa* metabolic network is less efficient for production of EPS than *R. solanacearum* (Table 4 and Data Set S2), with an increase of losses as CO₂ (+16%). In other words, biosynthesis of this virulence factor has a higher carbon cost in *X. fastidiosa* and this probably impairs reallocation of carbon fluxes to sustain efficient biomass production.

DISCUSSION

Fastidious growth is a paradoxical property of some prokaryote pathogens, and we sought to understand the emergence of this phenotype through a metabolic network study in a particularly fastidious organism, the plant pathogen *X. fastidiosa*. This bacterium appears to possess a minimal but fully functional metabolic network, and this was confirmed experimentally. This is in contrast with several other pathogen or symbiont species which have also undergone reductive evolution with the loss of essential metabolic functions (12, 46, 47).

The reduction of the *X. fastidiosa* metabolic network probably results from its adaptation to a limited number of environments. The reduction of the metabolic network does not create any auxotrophy for *X. fastidiosa* growth but tends to restrict the pathogen to a limited diversity of metabolic behaviors. *X. fastidiosa* is specifically restricted to two environments (plant vascular vessels and the foregut of xylem-eating insects) (15). These environments have common features as they are both constituted of xylem sap and carbonated polymers (plant cell wall and chitin), and it has been shown that the chitin-degrading enzyme is essential for colonization both in the insect and *in planta* (45). Thereby, *X. fastidiosa* appears to be restricted to a homeostatic environment, i.e., overall constant in composition and not prone to external perturbations. This lifestyle restricted to specific environments probably explains the limitation of metabolic behaviors (particularly the catabolic capacities), which was inferred from our study.

One could argue that fastidiousness of *Xylella* may be due to an environment poor in nutrients. However, *Xylella* has a fastidious growth even in nutrient-rich artificial media (e.g., buffered charcoal yeast extract [BCYE] medium [21]). In addition, other vascular plant pathogens such as *R. solanacearum* have a high proliferation rate in the same environment: 3 days after injection in stems, *R. solanacearum* can reach up to 10⁹ CFU per gram of fresh weight (48). Thereby, slow growth cannot be explained by a nutritional limitation *in planta* but seems to be due to intrinsic specificities of the pathogen.

The genome-scale metabolic analysis reveals a lack of metabolic robustness. Robustness is a key feature of biological systems, which allows them to maintain their function(s) when subjected to environmental or internal perturbation (7, 49). Genome-scale analysis of *X. fastidiosa* metabolism was carried out to examine if robustness could have shaped the evolution of its ancestor. By studying gene essentiality and enzyme distribution, we showed that functional redundancy, one of the main sources of robustness, is substantially missing in the *X. fastidiosa* metabolic network. This lack of robustness reduces the possibilities for *X. fastidiosa* to protect itself against perturbations both internal as mutations and external as environmental perturbations. FVA showed that the network lacks flexibility, and as mentioned above, this lack of robustness is also characterized by restricted trophic capabilities. This global fragility certainly makes *X. fastidiosa* very sensitive to deleterious mutations. The high level of homologous recombination observed in the species (50, 51) could serve as a rescue mechanism in this context.

Metabolic peculiarities responsible for a slow-growth phenotype. Several elements were raised by our study (Fig. 2).

(i) *X. fastidiosa* metabolism lacks certain genes/pathways which are not responsible for auxotrophy but are nevertheless assumed to ensure rapid growth.

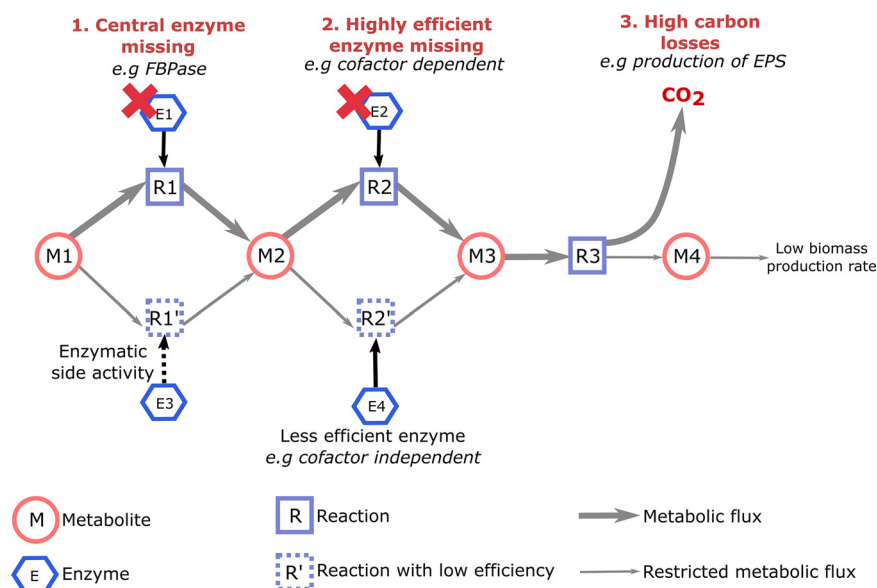


FIG 2 Metabolic properties contributing to fastidious growth. The three main metabolic properties unraveled by our study and probably contributing to fastidious growth are listed in red at the top of the figure. These three properties limit the metabolic fluxes. For 1 and 2, as the highly efficient enzyme is not available, a less efficient enzyme performs the reaction, which decreases the metabolic fluxes. For 3, the production of virulence factor strongly enhances carbon losses as CO₂, which will limit the ability of the network to efficiently convert substrate into biomass. These flux limitations are predicted to strongly reduce growth rate and be responsible, possibly with additional inputs such as regulation, for fastidious growth.

Some peripheral biosynthetic pathways appear to be missing, such as the ones for cobalamin and molybdopterin. It limits the bacterium to cobalamin- and molybdopterin-independent enzymes, usually possessing a lower enzymatic activity (52, 53). Similar observations were made on the respiratory metabolism, which appears to be restricted to a combination of poorly efficient cytochrome and cytochrome oxidase. A central enzyme, succinate dehydrogenase, also involved in respiratory metabolism, surprisingly lacks a membrane subunit, which could also affect the efficiency of central metabolic fluxes.

Furthermore, *X. fastidiosa* lacks two key enzymes: fructose-1,6-bisphosphatase (FBPase) for gluconeogenesis and transaldolase in the pentose phosphate pathway. We found that these lacks were not deleterious, suggesting that for FBPase the reaction was processed by a nonidentified route. The emerging concept of underground metabolism provides a reasonable hypothesis: the missing reaction could be achieved through the side activity of another enzyme, which leads to a reduced enzymatic activity (54).

A reduction in enzymatic activity in a reaction central for growth is assumed to strongly reduce the proliferation rate. To illustrate this phenomenon, we estimated that the experimentally observed *X. fastidiosa* growth rate (0.1608 day⁻¹) (19) was recovered *in silico* with a 3.37-fold reduction of the optimal FBPase flux (see Data Set S2 in the supplemental material). This reduction converted the generation time from 1.45 h (typical optimal bacterial growth) to 103 h (fastidious growth), so the growth rate is reduced by 71-fold, while the FBPase flux is reduced by only 3.37-fold. This *in silico* reduction seems reasonable, as higher flux reductions were experimentally observed (see, for example, a 200-fold reduction for an enzymatic activity in reference 54).

In photosynthetic organisms, a double role of sedoheptulose-1,7-bisphosphatase (SBPase) and FBPase activity in the same enzyme was reported, reinforcing the view that FBPase activity could be achieved by an alternative enzyme, with a lower efficiency (55–57). No SBPase exists in nonphotosynthetic organisms, but we hypothesize that another enzyme, *myo*-inositol 1-phosphatase (IMPase), could have a bisphosphatase

activity on fructose-1,6-bisphosphate. This IMPase enzyme (EC 3.1.3.25) was identified in the *X. fastidiosa* metabolic network. Although *myo*-inositol is not a hexose, it is a 6-carbon cyclic molecule with hydroxyl groups, which makes its chemical structure very similar to fructose. An enzyme with dual IMPase/FBPase activity was found in archaea (58) and also in the slow-growing pathogen *Mycobacterium tuberculosis* (59). It was shown that the archaeal IMPase had a catalytic activity on fructose-1,6-bisphosphate 3-fold lower than a classical FBPase (21 s^{-1} versus 7 s^{-1}) (58). Remarkably, the difference of activity measured in that study (3-fold) is similar to the loss of enzymatic efficiency we predicted to match fastidious growth (reduction of flux: 3.37-fold).

The loss of FBPase is observed among all *X. fastidiosa* strains sequenced to date. This observation suggests that this enzyme was already lost in the *Xylella* ancestor, whereas this enzyme (EC 3.1.3.11) is broadly conserved in living organisms (60). Looking more closely at the *Xanthomonadaceae* phylum to which *Xylella* belongs, it appears that FBPase is conserved in all *Xanthomonas* species except *Xanthomonas albilineans*. Interestingly, *X. albilineans* is also a xylem-limited and slow-growing plant pathogen that has undergone reductive evolution, although less extensively than *X. fastidiosa* (61). Future investigations should address whether the loss of FBPase is linked to a specialization in terms of environment or lifestyle.

(ii) *X. fastidiosa* metabolism is structurally inefficient. The decreased metabolic efficiency (in terms of yield) was particularly obvious in comparison with another vascular plant pathogen, *R. solanacearum*, when we determined the cost for the production and excretion of EPS, a major virulence factor of these bacteria (24, 62). In *R. solanacearum*, it was shown that EPS production has a significant metabolic cost that can impact biomass production (loss of approximately 25% of the growth rate due to EPS production) (22). Our simulations (Table 4) predict that the cost for EPS production is an even higher burden for *X. fastidiosa*.

Fastidious growth probably results from a combination of two factors. First is the lack of reactions catalyzed by efficient enzymes, cobalamin/molybdopterin-dependent enzymes, complete succinate dehydrogenase complex, efficient respiratory chain, and, strikingly, the absence of a central enzyme in gluconeogenesis. Second is a global inefficiency in producing virulence factors. We cannot formally exclude that enzymatic efficiency could be globally lower in *Xylella* species than in other bacteria. Surprisingly, the predictions from the efficiency analysis indicate that the potential for biomass production by *X. fastidiosa* is virtually similar to that of *R. solanacearum* (Table 4). This observation suggests that constraints imposed on metabolic efficiency both by virulence factor production and by regulation patterns specifically limit the growth of *X. fastidiosa*. Supporting this hypothesis, it was reported that an *X. fastidiosa* mutant deficient for the production of a secreted and virulence-related protein had a growth rate significantly increased in comparison to the wild-type strain (63). In such a scenario, the fastidious behavior could be viewed as a developmental strategy of the pathogen to remain at a low population level inside the host and avoid detection by its immune system. This hypothesis is in agreement with the view of *Xylella* as a “self-limiting” organism, which has many features of a plant commensal but accidentally provokes epidemics due to an exaggerated and late plant response (64), probably linked to specific environmental conditions.

Common metabolic peculiarities in fastidious pathogens. It is interesting to put these findings in relation to other fastidious organisms. The pathogen *B. pertussis*, similarly to *X. fastidiosa*, experienced a strong genome reduction, which implied a metabolic network reduction, leading to a number of reactions and metabolites close to *X. fastidiosa* (Table 1). The fastidious growth of *B. pertussis* could thus also be related to a lack of functional redundancy favoring less efficient pathways, and it is also conceivable that this reduction could affect the network efficiency and increase the cost of virulence factor production. Furthermore, another core metabolic enzyme is missing in *B. pertussis*, making its glycolysis unachievable (12). In contrast to *X. fastidiosa*, this absence led to an auxotrophy for amino acids, but one can consider that this

absence also constrains the metabolic fluxes and provokes fastidious growth. Another fastidious pathogen, *M. tuberculosis*, has an interesting similarity to *X. fastidiosa*; the lack of standard fructose-1,6-bisphosphatase was also reported in the pathogen, suggesting the use of an enzyme side activity (59) or an atypical fructose-1,6-bisphosphatase enzyme (65). These common metabolic particularities between slow-growing pathogens might indicate that in an environment where fast growth could activate the host immune system, similar evolutionary processes of growth reduction, at different degrees and strengths, might favor the emergence of fastidious phenotypes.

In conclusion, based on genetic and phenotypic data and computational approaches, we were able to unravel several candidate genes responsible for bacterial fastidious growth. A perspective of this study is to validate these candidates by functional genetic approaches to establish their involvement in the fastidious growth phenotype.

MATERIALS AND METHODS

Bacterial strain. Analyses were conducted with the strain CFBP 8418, an *X. fastidiosa* subsp. *multiplex* ST6 (sequence type 6) strain isolated from *Spartium junceum* in Alata (France) (23) and provided by the French Collection for Plant-associated Bacteria (CIRM-CFBP).

Carbon substrate phenotyping. Phenotyping was performed using Biolog phenotype microarray plates PM1 and PM2A according to the manufacturer's protocol, except that Tween 40 was replaced by Tween 80. An initial optical density (OD) of 0.18 (600 nm) was used for inoculation. Incubation time was 72.5 h. Three independent replicates were performed.

Growth was assumed proportional to respiration and was assessed by calculating the area under the curve (AUC) and the slope of the logarithm on the exponential phase (respiration rate). Growth was considered effective if $AUC > AUC_{\text{negative control}} + \text{threshold}$ (see Data Set S3). If the respiration rate was above 0.125 h^{-1} , the growth was categorized as fast (+ +); otherwise, it was categorized as slow (+). If the results were nonreproducible, the growth was assessed to be undetermined. For six substrates (out of 190), for which growth was assessed unambiguously as positive for two out of the three replicates, growth was referred to (+). The complete results are available in Data Set S3.

Genome-scale metabolic network reconstruction. The genome-scale metabolic network reconstruction was performed from the genomic sequences of the strain CFBP 8418 (GenBank accession no. [LUYA00000000.1](https://www.ncbi.nlm.nih.gov/nuccore/LUYA00000000.1)) (23). The protocol to generate high-quality genome-scale metabolic network proposed by Thiele and Palsson (66) was followed.

For the automatic reconstruction, the genomic sequences were compared, by priority order, to the five following metabolic models: *Escherichia coli* K-12 MG1655 (iJO1366 [67]), *Ralstonia solanacearum* GM11000 (iRP1476 [22]), *Pseudomonas aeruginosa* PAO1 (iMO1086 [68]), *Ralstonia eutropha* H16 (RehM-BEL1391 [69]), and *Bacillus subtilis* 168 (iYO844 [70]). *X. fastidiosa* sequences were compared by orthology to the sequences from each metabolic model, generating five draft models, thanks to the Autograph method (71). The SAMIR tool (22) was used to reconcile the identifiers between the models. Finally, the five metabolic models were merged into one draft model expressed with BiGG identifiers (72), following the priority order stated above and depending on the orthology quality.

The draft metabolic model was manually curated, evaluating the reactions one by one. The accuracy of each reaction was checked using KEGG (60), BiGG (72), BioCyc (73), MetaCyc (73), and bibliographical searches. Simulations (see below) were performed pathway by pathway to check if the curated pathway was functional. A manual gap-filling step was processed for nonfunctional pathways, looking for evidence of the missing reactions. Each reaction was scored to assess its reliability with a specific score that was more adapted to the network than the confidence score proposed by Thiele and Palsson (66). The meaning of this specific score and the complete manual curation protocol are available in Text S2. The two scores are given for each reaction in the metabolic network (Data Set S1).

As proposed by Thiele and Palsson (66), a biomass objective function was defined. General characterizations of the *X. fastidiosa* genome (29) and specificities of the studied strain (23) were both used. For missing information, data from *Xanthomonas campestris* pv. *campestris* (74) and *E. coli* (67) were used (Data Set S2). After curation, the tool CarveMe (75) was used to find other potential reactions. The generated reactions were manually curated and added to the network.

For metabolic network comparisons between subspecies, draft metabolic networks of *Xylella fastidiosa* subsp. *pauca* 9a5c (GenBank accession no. [GCA_000006725.1](https://www.ncbi.nlm.nih.gov/nuccore/GCA_000006725.1)) (29) and *X. fastidiosa* subsp. *fastidiosa* Temecula1 (GenBank accession no. [GCA_000007245.1](https://www.ncbi.nlm.nih.gov/nuccore/GCA_000007245.1)) (30) were generated with the same reconstruction process.

Comparative analysis. The reaction identifiers were given as input of the comparative analysis between *E. coli*, *R. solanacearum*, and *X. fastidiosa*. The metabolic model considered for *E. coli* was the model iJO1366 (67). For *R. solanacearum*, the model iRP1476 (22) was used, taking into account only the metabolic module. The Venn diagram was generated using the online tool BioVenn (76). The list of reactions in each part of the diagram is available in Data Set S2.

Computational simulations. To test the functionality of pathways and of the global network, simulations were performed on the model. To access intracellular fluxes and growth rate, the flux balance analysis (FBA) methodology was used (77). The constraints used to model the system are detailed in Text S3. To access the variability of each flux, flux variability analysis (FVA), a methodology based upon the

same principles, was then performed (78). A deviation of 1% from the optimality was allowed. *In silico* gene essentiality analysis was performed through multiple FBAs on the network. For each FBA, a metabolic gene of the network is deleted to test if its deletion has an impact on the organism growth. The *in silico* gene essentiality analysis in a protein-rich environment was inspired by a *B. pertussis* publication (12): L-glutamate as the major carbon source and an availability 10 times smaller in number of carbon for each other proteinogenic amino acid. For FVA and *in silico* gene essentiality, protein and EPS constraints were removed.

The structural efficiency of the network was tested in *X. fastidiosa* and, as a comparison, in *R. solanacearum*. To avoid bias, all the constraints were removed, and a generic L-glutamine uptake rate of $1 \text{ mmol}\cdot\text{h}^{-1}\cdot\text{g}$ (dry weight [DW])⁻¹ was used. Each of the biological processes (biomass and virulence) was studied separately, and the maximization of their synthesis was used as the objective. Each simulation result gave access to the proportion of carbon lost in the form of CO₂, with the exported CO₂ rate (R_EX_CO2_e). This allowed us to determine the maximal amount of carbon which could be dedicated to a virulence factor or biomass production. Metabolic yields, and consequently cost of virulence factors, were computed as the ratio between maximal production rate and the uptake rate, normalized by the number of carbons.

Text S4 provides a detailed description of mathematical modeling of metabolism used in the study.

Simulations were performed with the open source tool FlexFlux (79) and are reproducible using the guide provided in Text S4. The linear programming solver CPLEX, developed by IBM, was used to solve the system and get solutions. Scripts and command lines are available online on GitHub: <https://github.com/lgerlin/xfas-metabolic-model>.

Data availability. All data generated or analyzed during this study are included in figures or tables or in the supplemental material. In particular, raw data from Biolog phenotype microarray plates (for carbon substrate phenotyping) are available in Data Set S3.

Model and code availability. The *X. fastidiosa* subsp. *multiplex* strain CFBP 8418 metabolic model was named Xfm1158. The metabolic model was deposited in BioModels (80) and assigned the identifier MODEL2003100001. Exploration, omics mapping, and basic flux analyses can be performed on the model in MetExplore (81) (<https://metexplore.toulouse.inrae.fr/metexplore2/?idBioSource=5822>). The main scripts and command lines used for the study are available on GitHub: <https://github.com/lgerlin/xfas-metabolic-model>.

SUPPLEMENTAL MATERIAL

Supplemental material is available online only.

TEXT S1, TXT file, 2.5 MB.

TEXT S2, PDF file, 0.4 MB.

TEXT S3, PDF file, 0.3 MB.

TEXT S4, PDF file, 0.9 MB.

TABLE S1, PDF file, 0.6 MB.

TABLE S2, PDF file, 0.6 MB.

DATA SET S1, XLSX file, 0.2 MB.

DATA SET S2, XLSX file, 0.2 MB.

DATA SET S3, XLSX file, 0.9 MB.

DATA SET S4, XLSX file, 0.3 MB.

ACKNOWLEDGMENTS

L.G. was funded by a grant from the French Ministry of National Education and Research. The study was funded by the European Union's Horizon 2020 research and innovation program through grant agreement XF-ACTORS (727987) and the "Laboratoire d'Excellence (LABEX)" TULIP (ANR-10-LABX-41). The views expressed are purely those of the writers, and the EU funding agency is not responsible for any use that may be made of the information it contains. The funders had no role in study design, data collection and analysis, decision to publish, or preparation of the manuscript.

We acknowledge CIRM-CFBP (Beaucouzé, INRAE, France; http://www6.inrae.fr/cirm_eng/CFBP-Plant-Associated-Bacteria) for strain preservation and supply and access to the Omnilog station.

The authors declare that they have no competing interests.

Conceptualization: L.C., S.G., C.B. Metabolic reconstruction and curation: L.G., L.C. Simulations and analysis: L.G., C.B. Experiments: G.T., S.C. Funding acquisition: M.-A.J., S.G. Supervision: C.B. Writing—original draft: L.G. Writing—review & editing: L.G., C.B., L.C., G.T., S.C., M.-A.J., S.G.

REFERENCES

- Ibarra RU, Edwards JS, Palsson BO. 2002. *Escherichia coli* K-12 undergoes adaptive evolution to achieve in silico predicted optimal growth. *Nature* 420:186–123. <https://doi.org/10.1038/nature01149>.
- Edwards JS, Palsson BO. 1999. Systems properties of the *Haemophilus influenzae* Rd metabolic genotype. *J Biol Chem* 274:17410–17416. <https://doi.org/10.1074/jbc.274.25.17410>.
- Lewis NE, Hixson PK, Conrad TM, Lerman JA, Charusanti P, Polpitiya AD, Adkins JN, Schramm G, Purvine SO, Lopez-Ferrer D, Weitz KK, Eils R, König R, Smith RD, Palsson B. 2010. Omic data from evolved *E. coli* are consistent with computed optimal growth from genome-scale models. *Mol Syst Biol* 6:390. <https://doi.org/10.1038/msb.2010.47>.
- Guidot A, Jiang W, Ferdy JB, Thébaud C, Barberis P, Gouzy J, Genin S. 2014. Multihost experimental evolution of the pathogen *Ralstonia solanacearum* unveils genes involved in adaptation to plants. *Mol Biol Evol* 31:2913–2928. <https://doi.org/10.1093/molbev/msu229>.
- Perrier A, Peyraud R, Rengel D, Barlet X, Lucasson E, Gouzy J, Peeters N, Genin S, Guidot A. 2016. Enhanced in planta fitness through adaptive mutations in EfpR, a dual regulator of virulence and metabolic functions in the plant pathogen *Ralstonia solanacearum*. *PLoS Pathog* 12:e1006044–23. <https://doi.org/10.1371/journal.ppat.1006044>.
- Deslandes L, Genin S. 2014. Opening the *Ralstonia solanacearum* type III effector tool box: insights into host cell subversion mechanisms. *Curr Opin Plant Biol* 20:110–117. <https://doi.org/10.1016/j.pbi.2014.05.002>.
- Peyraud R, Cottret L, Marmiesse L, Genin S. 2018. Control of primary metabolism by a virulence regulatory network promotes robustness in a plant pathogen. *Nat Commun* 9:418. <https://doi.org/10.1038/s41467-017-02660-4>.
- Ribet D, Cossart P. 2015. How bacterial pathogens colonize their hosts and invade deeper tissues. *Microbes Infect* 17:173–183. <https://doi.org/10.1016/j.micinf.2015.01.004>.
- Doern GV. 2000. Detection of selected fastidious bacteria. *Clin Infect Dis* 30:166–173. <https://doi.org/10.1086/313586>.
- Thalen M, van den IJssel J, Jiskoot W, Zomer B, Roholl P, de Gooijer C, Beuvers C, Tramper J. 1999. Rational medium design for *Bordetella pertussis*: basic metabolism. *J Biotechnol* 75:147–159. [https://doi.org/10.1016/s0168-1656\(99\)00155-8](https://doi.org/10.1016/s0168-1656(99)00155-8).
- Kilgore PE, Salim AM, Zervos MJ, Schmitt H. 2016. Pertussis: microbiology, disease, treatment, and prevention. *Clin Microbiol Rev* 29:449–486. <https://doi.org/10.1128/CMR.00083-15>.
- Fyson N, King J, Belcher T, Preston A, Colijn C. 2017. A curated genome-scale metabolic model of *Bordetella pertussis* metabolism. *PLoS Comput Biol* 13:e1005639–17. <https://doi.org/10.1371/journal.pcbi.1005639>.
- James BW, Williams A, Marsh PD. 2000. The physiology and pathogenicity of *Mycobacterium tuberculosis* grown under controlled conditions in a defined medium. *J Appl Microbiol* 88:669–677. <https://doi.org/10.1046/j.1365-2672.2000.01020.x>.
- Edelstein PH. 2000. Detection of selected fastidious bacteria. *Clin Infect Dis* 31:846. <https://doi.org/10.1086/314002>.
- Sicard A, Zeilinger AR, Vanhove M, Schartel TE, Beal DJ, Daugherty MP, Almeida R. 2018. *Xylella fastidiosa*: insights into an emerging plant pathogen. *Annu Rev Phytopathol* 56:181–202. <https://doi.org/10.1146/annurev-phyto-080417-045849>.
- Rapicavoli J, Ingel B, Blanco-Ulate B, Cantu D, Roper C. 2018. *Xylella fastidiosa*: an examination of a re-emerging plant pathogen. *Mol Plant Pathol* 19:786–800. <https://doi.org/10.1111/mpp.12585>.
- European and Mediterranean Plant Protection Organization. 2016. PM 7/24 (2) *Xylella fastidiosa*. *EPPO Bull* 46:463–500. <https://doi.org/10.1111/epp.12327>.
- Lemos E, Alves LMC, Campanharo JC. 2003. Genomics-based design of defined growth media for the plant pathogen *Xylella fastidiosa*. *FEMS Microbiol Lett* 219:39–45. [https://doi.org/10.1016/S0378-1097\(02\)01189-8](https://doi.org/10.1016/S0378-1097(02)01189-8).
- Leite B, Andersen PC, Ishida ML. 2004. Colony aggregation and biofilm formation in xylem chemistry-based media for *Xylella fastidiosa*. *FEMS Microbiol Lett* 230:283–290. [https://doi.org/10.1016/S0378-1097\(03\)00917-0](https://doi.org/10.1016/S0378-1097(03)00917-0).
- Almeida RPP, Mann R, Purcell AH. 2004. *Xylella fastidiosa* cultivation on a minimal solid defined medium. *Curr Microbiol* 48:368–372. <https://doi.org/10.1007/s00284-003-4219-x>.
- Shriner AD, Andersen PC. 2014. Effect of oxygen on the growth and biofilm formation of *Xylella fastidiosa* in liquid media. *Curr Microbiol* 69:866–873. <https://doi.org/10.1007/s00284-014-0660-2>.
- Peyraud R, Cottret L, Marmiesse L, Gouzy J, Genin S. 2016. A resource allocation trade-off between virulence and proliferation drives metabolic versatility in the plant pathogen *Ralstonia solanacearum*. *PLoS Pathog* 12:e1005939. <https://doi.org/10.1371/journal.ppat.1005939>.
- Denancé N, Legendre B, Briand M, Olivier V, de Boisseson C, Poliakov F, Jacques MA. 2017. Several subspecies and sequence types are associated with the emergence of *Xylella fastidiosa* in natural settings in France. *Plant Pathol* 66:1054–1064. <https://doi.org/10.1111/ppa.12695>.
- Da Silva FR, Vettore AL, Kemper EL, Leite A, Arruda P. 2001. Fastidious gum: the *Xylella fastidiosa* exopolysaccharide possibly involved in bacterial pathogenicity. *FEMS Microbiol Lett* 203:165–171. <https://doi.org/10.1111/j.1574-6968.2001.tb10836.x>.
- Clifford JC, Rapicavoli JN, Roper MC. 2013. A rhamnose-rich O-antigen mediates adhesion, virulence, and host colonization for the xylem-limited phytopathogen *Xylella fastidiosa*. *Mol Plant Microbe Interact* 26:676–685. <https://doi.org/10.1094/MPMI-12-12-0283-R>.
- Rapicavoli JN, Blanco-Ulate B, Muszyński A, Figueroa-Balderas R, Morales-Cruz A, Azadi P, Dobruchowska JM, Castro C, Cantu D, Roper MC. 2018. Lipopolysaccharide O-antigen delays plant innate immune recognition of *Xylella fastidiosa*. *Nat Commun* 9:390. <https://doi.org/10.1038/s41467-018-02861-5>.
- Nascimento R, Gouran H, Chakraborty S, Gillespie HW, Almeida-Souza HO, Tu A, Rao BJ, Feldstein PA, Bruening G, Goulart LR, Dandekar AM. 2016. The type II secreted lipase/esterase LesA is a key virulence factor required for *Xylella fastidiosa* pathogenesis in grapevines. *Sci Rep* 6:18598. <https://doi.org/10.1038/srep18598>.
- Bucci EM. 2018. *Xylella fastidiosa*, a new plant pathogen that threatens global farming: ecology, molecular biology, search for remedies. *Biochem Biophys Res Commun* 502:173–182. <https://doi.org/10.1016/j.bbrc.2018.05.073>.
- Simpson AJG, Reinach FC, Arruda P, Abreu FA, Acencio M, Alvarenga R, Alves LMC, Araya JE, Baia GS, Baptista CS, Barros MH, Bonaccorsi ED, Bordin S, Bové JM, Briones MRS, Bueno MRP, Camargo AA, Camargo LEA, Carraro DM, Carrer H, Colauto NB, Colombo C, Costa FF, Costa MCR, Costa-Neto CM, Coutinho LL, Cristofani M, Dias-Neto E, Docena C, El-Dorry H, Facincani AP, Ferreira AJ, Ferreira VCA, Ferro JA, Fraga JS, França SC, Franco MC, Frohne M, Furlan LR, Garnier M, Goldman GH, Goldman MHS, Gomes SL, Gruber A, Ho PL, Hoheisel JD, Junqueira ML, Kemper EL, Kitajima JP, Krieger JE, Kuramae EE, Laigret F, Lambais MR, Leite LCC, Lemos E, Lemos MVF, Lopes SA, Lopes CR, Machado JA, Machado MA, Madeira A, Madeira HMF, Marino CL, Marques MV, Martins EAL, Martins EMF, Matsukuma AY, Menck CFM, Miracca EC, Miyaki CY, Monteiro-Vitorello CB, Moon DH, Nagai MA, Nascimento A, Netto LES, Nhani A, Nobrega FG, Nunes LR, Oliveira MA, de Oliveira MC, de Oliveira RC, Palmieri DA, Paris A, Peixoto BR, Pereira GAG, Pereira HA, Pesquero JB, Quaggio RB, Roberto PG, Rodrigues V, de M, Rosa AJ, de Rosa VE, de Sá RG, Santelli RV, Sawasaki HE, da Silva ACR, da Silva AM, da Silva FR, Silva WA, da Silveira JF, Silvestri MLZ, Siqueira WJ, de Souza AA, de Souza AP, Terenzi MF, Truffi D, Tsai SM, Tshako MH, Vallada H, Van Sluys MA, Verjovski-Almeida S, Vettore AL, Zago MA, Zatz M, Meidanis J, Setubal JC. 2000. The genome sequence of the plant pathogen *Xylella fastidiosa*. *Nature* 406:151–157. <https://doi.org/10.1038/35018003>.
- Van Sluys MA, de Oliveira MC, Monteiro-Vitorello CB, Miyaki CY, Furlan LR, Camargo LEA, da Silva ACR, Moon DH, Takita MA, Lemos EGM, Machado MA, Ferro MIT, da Silva FR, Goldman MHS, Goldman GH, Lemos MVF, El-Dorry H, Tsai SM, Carrer H, Carraro DM, de Oliveira RC, Nunes LR, Siqueira WJ, Coutinho LL, Kimura ET, Ferro ES, Harakava R, Kuramae EE, Marino CL, Giglioti E, Abreu IL, Alves LMC, do Amaral AM, Baia GS, Blanco SR, Brito MS, Cannavan FS, Celestino AV, da Cunha AF, Fenille RC, Ferro JA, Formighieri EF, Kishi LT, Leoni SG, Oliveira AR, Rosa VE, Sasaki FT, Sena JAD, de Souza AA, Truffi D, Tsukumo F, Yanai GM, Zarus LG, Civerolo EL, Simpson AJG, Almeida NF, Setubal JC, Kitajima JP. 2003. Comparative analyses of the complete genome sequences of Pierce's disease and citrus variegated chlorosis strains of *Xylella fastidiosa*. *J Bacteriol* 185:1018–1026. <https://doi.org/10.1128/jb.185.3.1018-1026.2003>.
- O'Reilly C, Turner PD. 2003. The nitrilase family of CN hydrolysing enzymes—a comparative study. *J Appl Microbiol* 95:1161–1174. <https://doi.org/10.1046/j.1365-2672.2003.02123.x>.
- Camejo D, Guzmán-Cedeño Á, Moreno A. 2016. Reactive oxygen species, essential molecules, during plant-pathogen interactions. *Plant Physiol Biochem* 103:10–23. <https://doi.org/10.1016/j.plaphy.2016.02.035>.
- Howden AJM, Preston GM. 2009. Nitrilase enzymes and their role in

- plant-microbe interactions. *Microb Biotechnol* 2:441–451. <https://doi.org/10.1111/j.1751-7915.2009.00111.x>.
34. Rodionov DA, Vitreschak AG, Mironov AA, Gelfand MS. 2003. Comparative genomics of the vitamin B₁₂ metabolism and regulation in prokaryotes. *J Biol Chem* 278:41148–41159. <https://doi.org/10.1074/jbc.M305837200>.
 35. Bhattacharyya A, Stilwagen S, Reznik G, Feil H, Feil WS, Anderson I, Bernal A, D'Souza M, Ivanova N, Kapatral V, Larsen N, Los T, Lykidis A, Selkov E, Walunas TL, Purcell A, Edwards RA, Hawkins T, Haselkorn R, Overbeek R, Kyrpidis NC, Predki PF. 2002. Draft sequencing and comparative genomics of *Xylella fastidiosa* strains reveal novel biological insights. *Genome Res* 12:1556–1563. <https://doi.org/10.1101/gr.370702>.
 36. Hederstedt L, Heden LO. 1989. New properties of *Bacillus subtilis* succinate dehydrogenase altered at the active site. The apparent active site thiol of succinate oxidoreductases is dispensable for succinate oxidation. *Biochem J* 260:491–497. <https://doi.org/10.1042/bj2600491>.
 37. Andersen PC, Brodbeck BV. 1989. Diurnal and temporal changes in the chemical profile of xylem exudate from *Vitis rotundifolia*. *Physiol Plant* 75:63–70. <https://doi.org/10.1111/j.1399-3054.1989.tb02064.x>.
 38. Andersen PC, Brodbeck BV, Oden S, Shriner A, Leite B. 2007. Influence of xylem fluid chemistry on planktonic growth, biofilm formation and aggregation of *Xylella fastidiosa*. *FEMS Microbiol Lett* 274:210–217. <https://doi.org/10.1111/j.1574-6968.2007.00827.x>.
 39. Montes Borrego M, Jiménez-Díaz RM, Trapero Casas JL, Navas Cortés JA, Haro C, Rivas JC, de la Fuente L, Landa BB. 2017. Metabolomic characterization of xylem sap of different olive cultivars growing in Spain. *Eur Conf Xylella fastidiosa*, poster 2.6.
 40. Zuluaga AP, Puigvert M, Valls M. 2013. Novel plant inputs influencing *Ralstonia solanacearum* during infection. *Front Microbiol* 4:349. <https://doi.org/10.3389/fmicb.2013.00349>.
 41. Sedivy JM, Fraenkel DG. 1985. Fructose bisphosphatase of *Saccharomyces cerevisiae*. Cloning, disruption and regulation of the FBP1 structural gene. *J Mol Biol* 186:307–319. [https://doi.org/10.1016/0022-2836\(85\)90107-X](https://doi.org/10.1016/0022-2836(85)90107-X).
 42. Rittmann D, Schaffer S, Wendisch VF, Sahm H. 2003. Fructose-1,6-bisphosphatase from *Corynebacterium glutamicum*: expression and deletion of the *fbp* gene and biochemical characterization of the enzyme. *Arch Microbiol* 180:285–292. <https://doi.org/10.1007/s00203-003-0588-6>.
 43. Stinccone A, Prigione A, Cramer T, Wamelink MMC, Campbell K, Cheung E, Olin-Sandoval V, Grüning NM, Krüger A, Tauqeer Alam M, Keller MA, Breitenbach M, Brindle KM, Rabinowitz JD, Ralser M. 2015. The return of metabolism: biochemistry and physiology of the pentose phosphate pathway. *Biol Rev Camb Philos Soc* 90:927–963. <https://doi.org/10.1111/brv.12140>.
 44. Yoon SH, Han MJ, Jeong H, Lee CH, Xia XX, Lee DH, Shim JH, Lee SY, Oh TK, Kim JF. 2012. Comparative multi-omics systems analysis of *Escherichia coli* strains B and K-12. *Genome Biol* 13:R37. <https://doi.org/10.1186/gb-2012-13-5-r37>.
 45. Labroussaa F, Ionescu M, Zeilinger AR, Lindow SE, Almeida R. 2017. A chitinase is required for *Xylella fastidiosa* colonization of its insect and plant hosts. *Microbiology* 163:502–509. <https://doi.org/10.1099/mic.0.000438>.
 46. Fenn K, Blaxter M. 2006. *Wolbachia* genomes: revealing the biology of parasitism and mutualism. *Trends Parasitol* 22:60–65. <https://doi.org/10.1016/j.pt.2005.12.012>.
 47. Thomas GH, Zucker J, Macdonald SJ, Sorokin A, Goryanin I, Douglas AE. 2009. A fragile metabolic network adapted for cooperation in the symbiotic bacterium *Buchnera aphidicola*. *BMC Syst Biol* 3:24. <https://doi.org/10.1186/1752-0509-3-24>.
 48. Perrier A, Barlet X, Rengel D, Prior P, Poussier S, Genin S, Guidot A. 2019. Spontaneous mutations in a regulatory gene induce phenotypic heterogeneity and adaptation of *Ralstonia solanacearum* to changing environments. *Environ Microbiol* 21:3140–3152. <https://doi.org/10.1111/1462-2920.14717>.
 49. Félix M-A, Barkoulas M. 2015. Pervasive robustness in biological systems. *Nat Rev Genet* 16:483–496. <https://doi.org/10.1038/nrg3949>.
 50. Nunney L, Yuan X, Bromley RE, Stouthamer R. 2012. Detecting genetic introgression: high levels of intersubspecific recombination found in *Xylella fastidiosa* in Brazil. *Appl Environ Microbiol* 78:4702–4714. <https://doi.org/10.1128/AEM.01126-12>.
 51. Coletta-Filho HD, Francisco CS, Lopes JRS, Muller C, Almeida R. 2017. Homologous recombination and *Xylella fastidiosa* host-pathogen associations in South America. *Phytopathology* 107:305–312. <https://doi.org/10.1094/PHYTO-09-16-0321-R>.
 52. Schomburg I, Chang A, Ebeling C, Gremse M, Heldt C, Huhn G, Schomburg D. 2004. BRENDA, the enzyme database: updates and major new developments. *Nucleic Acids Res* 32:D431–D433. <https://doi.org/10.1093/nar/gkh081>.
 53. Plener L, Boistard P, González A, Boucher C, Genin S. 2012. Metabolic adaptation of *Ralstonia solanacearum* during plant infection: a methionine biosynthesis case study. *PLoS One* 7:e36877. <https://doi.org/10.1371/journal.pone.0036877>.
 54. Notebaart RA, Szappanos B, Kintsjes B, Pál F, Györkei Á, Bogos B, Lázár V, Spohn R, Csörgő B, Wagner A, Ruppín E, Pál C, Papp B. 2014. Network-level architecture and the evolutionary potential of underground metabolism. *Proc Natl Acad Sci U S A* 111:11762–11767. <https://doi.org/10.1073/pnas.1406102111>.
 55. Ding F, Wang M, Zhang S, Ai X. 2016. Changes in SBPase activity influence photosynthetic capacity, growth, and tolerance to chilling stress in transgenic tomato plants. *Sci Rep* 6:32741. <https://doi.org/10.1038/srep32741>.
 56. Gerbling K-P, Steup M, Latzko E. 1986. Fructose 1,6-bisphosphatase form B from *Synechococcus leopoliensis* hydrolyzes both fructose and sedoheptulose bisphosphate. *Plant Physiol* 80:716–720. <https://doi.org/10.1103/pp.80.3.716>.
 57. Jiang Y-H, Wang D-Y, Wen J-F. 2012. The independent prokaryotic origins of eukaryotic fructose-1,6-bisphosphatase and sedoheptulose-1,7-bisphosphatase and the implications of their origins for the evolution of eukaryotic Calvin cycle. *BMC Evol Biol* 12:208. <https://doi.org/10.1186/1471-2148-12-208>.
 58. Stec B, Yang H, Johnson KA, Chen L, Roberts MF. 2000. MJ0109 is an enzyme that is both an inositol monophosphatase and the “missing” archaeal fructose-1,6-bisphosphatase. *Nat Struct Biol* 7:1046–1050. <https://doi.org/10.1038/80968>.
 59. Gu X, Chen M, Shen H, Jiang X, Huang Y, Wang H. 2006. Rv2131c gene product: an unconventional enzyme that is both inositol monophosphatase and fructose-1,6-bisphosphatase. *Biochem Biophys Res Commun* 339:897–904. <https://doi.org/10.1016/j.bbrc.2005.11.088>.
 60. Kanehisa M, Furumichi M, Tanabe M, Sato Y, Morishima K. 2017. KEGG: new perspectives on genomes, pathways, diseases and drugs. *Nucleic Acids Res* 45:D353–D361. <https://doi.org/10.1093/nar/gkw1092>.
 61. Pieretti I, Royer M, Barbe V, Carrere S, Koebnik R, Cociancich S, Couloux A, Darrasse A, Gouzy J, Jacques M-A, Lauber E, Manceau C, Mangenot S, Poussier S, Segurens B, Szurek B, Verdier V, Arlat M, Rott P. 2009. The complete genome sequence of *Xanthomonas albilineans* provides new insights into the reductive genome evolution of the xylem-limited Xanthomonadaceae. *BMC Genomics* 10:616. <https://doi.org/10.1186/1471-2164-10-616>.
 62. Lowe-Power TM, Khokhani D, Allen C. 2018. How *Ralstonia solanacearum* exploits and thrives in the flowing plant xylem environment. *Trends Microbiol* 26:929–942. <https://doi.org/10.1016/j.tim.2018.06.002>.
 63. Gouran H, Gillespie H, Nascimento R, Chakraborty S, Zaini PA, Jacobson A, Phinney BS, Dolan D, Durbin-Johnson BP, Antonova ES, Lindow SE, Mellema MS, Goulart LR, Dandekar AM. 2016. The secreted protease PrtA controls cell growth, biofilm formation and pathogenicity in *Xylella fastidiosa*. *Sci Rep* 6:31098. <https://doi.org/10.1038/srep31098>.
 64. Roper C, Castro C, Ingel B. 2019. *Xylella fastidiosa*: bacterial parasitism with hallmarks of commensalism. *Curr Opin Plant Biol* 50:140–147. <https://doi.org/10.1016/j.cpb.2019.05.005>.
 65. Ganapathy U, Marrero J, Calhoun S, Eoh H, De Carvalho LPS, Rhee K, Ehrt S. 2015. Two enzymes with redundant fructose bisphosphatase activity sustain gluconeogenesis and virulence in *Mycobacterium tuberculosis*. *Nat Commun* 6:7912. <https://doi.org/10.1038/ncomms8912>.
 66. Thiele I, Palsson BØ. 2010. A protocol for generating a high-quality genome-scale metabolic reconstruction. *Nat Protoc* 5:93–121. <https://doi.org/10.1038/nprot.2009.203>.
 67. Orth JD, Conrad TM, Na J, Lerman JA, Nam H, Feist AM, Palsson BØ. 2011. A comprehensive genome-scale reconstruction of *Escherichia coli* metabolism—2011. *Mol Syst Biol* 7:535. <https://doi.org/10.1038/msb.2011.65>.
 68. Oberhardt MA, Puchalka J, Martins dos Santos VAP, Papin JA. 2011. Reconciliation of genome-scale metabolic reconstructions for comparative systems analysis. *PLoS Comput Biol* 7:e1001116. <https://doi.org/10.1371/journal.pcbi.1001116>.
 69. Park J, Kim T, Lee S. 2011. Genome-scale reconstruction and in silico analysis of the *Ralstonia eutropha* H16 for polyhydroxyalkanoate synthesis, lithoautotrophic growth, and 2-methyl citric acid production. *BMC Syst Biol* 5:101. <https://doi.org/10.1186/1752-0509-5-101>.
 70. Oh Y-K, Palsson BO, Park SM, Schilling CH, Mahadevan R. 2007. Genome-scale reconstruction of metabolic network in *Bacillus subtilis* based on

- high-throughput phenotyping and gene essentiality data. *J Biol Chem* 282:28791–28799. <https://doi.org/10.1074/jbc.M703759200>.
71. Notebaart RA, van Enkevort FH, Francke C, Siezen RJ, Teusink B. 2006. Accelerating the reconstruction of genome-scale metabolic networks. *BMC Bioinformatics* 7:296. <https://doi.org/10.1186/1471-2105-7-296>.
 72. King ZA, Lu J, Dräger A, Miller P, Federowicz S, Lerman JA, Ebrahim A, Palsson BO, Lewis NE. 2016. BiGG Models: a platform for integrating, standardizing and sharing genome-scale models. *Nucleic Acids Res* 44:D515–D522. <https://doi.org/10.1093/nar/gkv1049>.
 73. Caspi R, Billington R, Ferrer L, Foerster H, Fulcher CA, Keseler IM, Kothari A, Krummenacker M, Latendresse M, Mueller LA, Ong Q, Paley S, Subhraveti P, Weaver DS, Karp PD. 2016. The MetaCyc database of metabolic pathways and enzymes and the BioCyc collection of pathway/genome databases. *Nucleic Acids Res* 44:D471–D480. <https://doi.org/10.1093/nar/gkv1164>.
 74. Schatschneider S, Persicke M, Watt SA, Hublik G, Pühler A, Niehaus K, Vorhölter FJ. 2013. Establishment, in silico analysis, and experimental verification of a large-scale metabolic network of the xanthan producing *Xanthomonas campestris* pv. *campestris* strain B100. *J Biotechnol* 167: 123–134. <https://doi.org/10.1016/j.jbiotec.2013.01.023>.
 75. Machado D, Andrejev S, Tramontano M, Patil KR. 2018. Fast automated reconstruction of genome-scale metabolic models for microbial species and communities. *Nucleic Acids Res* 46:7542–7553. <https://doi.org/10.1093/nar/gky537>.
 76. Hulsen T, de Vlieg J, Alkema W. 2008. BioVenn—a web application for the comparison and visualization of biological lists using area-proportional Venn diagrams. *BMC Genomics* 9:488. <https://doi.org/10.1186/1471-2164-9-488>.
 77. Orth JD, Thiele I, Palsson BØ. 2010. What is flux balance analysis? *Nat Biotechnol* 28:245–248. <https://doi.org/10.1038/nbt.1614>.
 78. Mahadevan R, Schilling CH. 2003. The effects of alternate optimal solutions in constraint-based genome-scale metabolic models. *Metab Eng* 5:264–276. <https://doi.org/10.1016/j.ymben.2003.09.002>.
 79. Marmiesse L, Peyraud R, Cottret L. 2015. FlexFlux: combining metabolic flux and regulatory network analyses. *BMC Syst Biol* 9:93. <https://doi.org/10.1186/s12918-015-0238-z>.
 80. Glont M, Nguyen TVN, Graesslin M, Hälke R, Ali R, Schramm J, Wimalaratne SM, Kothamachu VB, Rodriguez N, Swat MJ, Eils J, Eils R, Laibe C, Malik-Sheriff RS, Chelliah V, Le Novère N, Hermjakob H. 2018. BioModels: expanding horizons to include more modelling approaches and formats. *Nucleic Acids Res* 46:D1248–D1253. <https://doi.org/10.1093/nar/gkx1023>.
 81. Cottret L, Frainay C, Chazalviel M, Cabanettes F, Gloaguen Y, Camenen E, Merlet B, Heux S, Portais J-C, Poupin N, Vinson F, Jourdan F. 2018. MetExplore: collaborative edition and exploration of metabolic networks. *Nucleic Acids Res* 46:W495–W502. <https://doi.org/10.1093/nar/gky301>.
 82. Navarrete F, De La Fuente L. 2014. Response of *Xylella fastidiosa* to zinc: decreased culturability, increased exopolysaccharide production, and formation of resilient biofilms under flow conditions. *Appl Environ Microbiol* 80:1097–1107. <https://doi.org/10.1128/AEM.02998-13>.